HHS Public Access

Author manuscript

Acta Biomater. Author manuscript; available in PMC 2018 September 15.

Published in final edited form as:

Acta Biomater. 2017 September 15; 60: 181–189. doi:10.1016/j.actbio.2017.07.017.

Hydrogel elasticity and microarchitecture regulate dental-derived mesenchymal stem cells -host immune system cross-talk

Sahar Ansari, PhD[1,#], **Chider Chen, PhD**[2,#], **Mohammad Mahdi Hasani-Sarabadi, PhD**[1], **Bo Yu, DDS, PhD**[1], **Homayoun H. Zadeh, DDS, PhD**[3], **Benjamin M Wu, DDS, PhD**[1], and **Alireza Moshaverinia, DDS, MS, PhD**[1,*]

[1]Weintraub Center for Reconstructive Biotechnology, Division of Advanced Prosthodontics, School of Dentistry, University of California, Los Angeles, CA

[2]Department of Anatomy & Cell Biology, School of Dental Medicine, University of Pennsylvania, Philadelphia, PA

[3]Ostrow School of Dentistry, University of Southern California, Los Angeles, CA

Abstract

The host immune system (T-lymphocytes and their pro-inflammatory cytokines) has been shown to compromise bone regeneration ability of mesenchymal stem cells (MSCs). We have recently shown that hydrogel, used as an encapsulating biomaterial affects the cross-talk among host immune cells and MSCs. However, the role of hydrogel elasticity and porosity in regulation of cross-talk between dental-derived MSCs and immune cells is unclear. In this study, we demonstrate that the modulus of elasticity and porosity of the scaffold influence T-lymphocyte-dental MSC interplay by regulating the penetration of inflammatory T cells and their cytokines. Moreover, we demonstrated that alginate hydrogels with different elasticity and microporous structure can regulate the viability and determine the fate of the encapsulated MSCs through modulation of NF-kB pathway. Our *in vivo* data show that alginate hydrogels with smaller pores and higher elasticity could prevent pro-inflammatory cytokine-induced MSC apoptosis by down-regulating the Caspase-3- and 8-associated proapoptotic cascades, leading to higher amounts of ectopic bone regeneration. Additionally, dental-derived MSCs encapsulated in hydrogel with higher elasticity exhibited lower expression levels of NF-kB p65 and Cox-2 *in vivo*. Taken together, our findings demonstrate that the mechanical characteristics and microarchitecture of the microenvironment encapsulating MSCs, in addition to presence of T-lymphocytes and their pro-inflammatory cytokines, affect the fate of encapsulated dental-derived MSCs.

[*]**Corresponding author:** Alireza Moshaverinia, DDS, MS, PhD, FACP, Assistant Professor, Diplomate, American Board of Prosthodontics, Division of Advanced Prosthodontics, UCLA School of Dentistry, 10833 LeConte Ave, B3-023 CHS, Los Angeles, California 90095-1668, amoshaverinia@ucla.edu, Tel: (310) 794-6324.

[#]These authors contributed equally to this work.

Graphical abstract

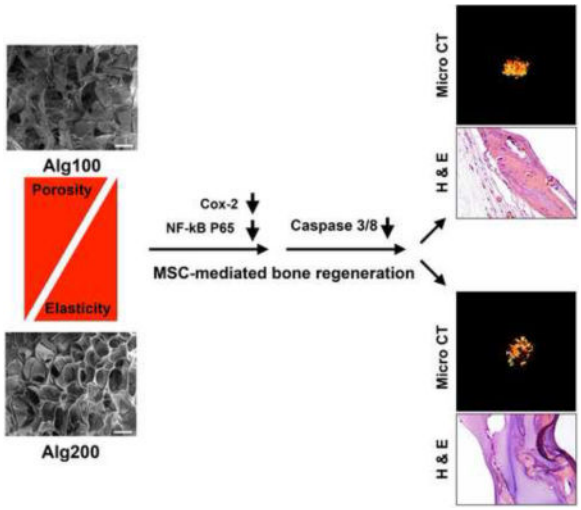

Keywords

Alginate hydrogel; porosity; elasticity; host immune system; bone tissue engineering

1. Introduction

Craniofacial bone tissue engineering currently relies extensively on bone grafting procedures [1–3]. However, there are numerous well-documented drawbacks related to this therapeutic approach [4–7]. Mesenchymal stem cells (MSCs) represent an alternative treatment modality in regenerative medicine.[4–10] MSCs derived from orofacial tissues (e.g., stem cells from human exfoliated deciduous teeth (SHED)) are attractive postnatal stem cells with desirable self-renewal capacity and plasticity and osteogenic properties comparable to bone marrow mesenchymal stem cells (BMMSCs) [10–17]. SHED are easily found in pediatric patient's mouth or in tissue waste in pediatric dental clinics. Preclinical and clinical investigations have revealed that SHED are able to generate new bone with great potential for bone repair/regeneration [15, 16]. Moreover, these cells are originated from neural crest that makes them particularly compatible for regeneration and repair of neural crest-derived tissues (e.g., jaw bone) [13–19]. Recent studies have emphasized, however, that the cell source is not the sole determinant of success in stem cell-mediated regenerative medicine. The host immune system can have an adverse effect on outcomes. For example, proinflammatory T-cells and cytokines inhibit MSC-mediated bone tissue regeneration [20–22]. These effects can be modulated by local administration of anti-inflammatory agents (e.g. aspirin or indomethacin), which have been shown to improve MSC-mediated bone regeneration [21,22].

The choice of carrier can also strongly affect the performance of MSCs in tissue engineering applications, in part due to immunomodulatory effects, and also because they offer the opportunity to direct the stem cells fate towards the desired phenotype [22–24]. However, regulation of the encapsulated MSCs' is still the main challenge. Hydrogel scaffolds have

been largely utilized to study the interaction of biomaterial and MSCs [25–28] RGD-coupled alginate hydrogel has been used extensively for cell encapsulation in bone tissue regeneration [27–32]. Alginate hydrogel can delay the penetration of the inflammatory cytokines and T cells, and act as a physical shield to protect the implanted MSCs from the immune cell attack [22]. Therefore, the scaffold material can affect the cross-talk between MSC and host immune cell, control the implanted MSCs fate, toward improved tissue regeneration quality. Furthermore, it is understood that physiomechanical properties including porosity of the biomaterial influence MSC differentiation, but their roles in the MSC-host immune interaction are fairly unknown [36]. There are no studies evaluating the role of porosity and elasticity of the biomaterial in MSC-proinflammatory T cell/cytokine interplay. How this interplay affects the bone regenerative properties of dental-derived MSCs in particular, has received little attention.

Understanding the factors influencing the fate of encapsulating MSCs is of major therapeutic interest [36]. To develop effective MSC-based regenerative therapies it is crucial to have a clear understanding of how the physiomechanical properties including porosity and elasticity of the encapsulating biomaterial affect the cross talk between the immune cells and MSCs. Hence, the main goal of our study was to clarify the role of mechanical properties and microarchitecture of the hydrogel biomaterial in directing the fate of encapsulated dental-derived MSCs toward osteogenic tissues.

2. Materials and methods

2.1. Cell isolation and culture

SHED were used and cultured according to published protocols [15,16] with required IRB approval. The pulp tissues were separated from exfoliated human primary upper and lower central or lateral incisors (isolated from twelve children aged 6–12) and then processed according to methods in the literature [15,16]. Mouse Pan T lymphocytes were isolated according to previously published protocols [21, 22] using a magnetic cell sorter (Pan T Cell Isolation Kit II, Miltenyi Biotec, San Diego, CA).

2.2. Biomaterial fabrication and cell encapsulation

High molecular weight RGD-modified alginate (NovaMatrix, Norway) was utilized as the encapsulating biomaterial [22,37,38]. The alginate was charcoal treated and oxidized. Subsequently, the hydrogel biomaterials were sterile filtered (0.22 μm filters, Millipore, Billerica, MA) prior to the cell encapsulation process. 2×10^6 SHED were encapsulated in 1 mL of 1.2 % w/v alginate hydrogel. Alginate microspheres were formed employing a microfluidic device and dropwise addition of alginate to $CaCl_2$ solutions with two concentrations: 100 or 200 mM. In order to generate biomaterials with different moduli of elasticity and, therefore, porosity, two different calcium ion concentrations (100 and 200 mM) were used. As the negative group, cell-free alginate hydrogel was utilized.

2.3. Characterization of the fabricated hydrogel scaffolds

The Young’s moduli of the fabricated alginate hydrogels were analyzed in accordance with previously published methods [39]. The cross-sectional microstructure of the prepared

alginate scaffolds were analyzed using scanning electron microscopy (SEM). Lyophilized hydrogels were freeze-fractured (using liquid nitrogen) to expose a cross-section. The scaffold specimens were imaged without further coating using a ZEISS Supra 40VP scanning electron microscope (Zeiss Microscopy GmbH, Jena, Germany). The porosity was further characterized using SEM images by evaluating at least 40 pores using the ImageJ program (National Institutes of Health, Bethesda, MD).

To determine the influence of the elasticity of the hydrogel on its permeability, the release profiles of Trypsin inhibitor (from turkey egg white, 20 kDa; Sigma), bovine serum albumin (BSA, 66 kDa; Sigma), and IgG (from rat serum, 150 kDa; Sigma) from alginate scaffolds were evaluated in PBS solution at different time points. Subsequently, UV spectrophotometer (at 320 nm, Beckman, Brea, CA) was utilized to analyze the amount of released protein for up to two weeks. Additionally, the permeability of the alginate hydrogels to TNF-α (BioLegend, San Diego CA) was evaluated. Briefly, alginate hydrogels were immersed in a 200 μg/mL solution of TNF-α. After 6, 12 and 24 hours, the diffused cytokine in the hydrogels was detected using fluorescent microscopy with anti-TNF-α antibodies (Abcam). Seven specimens (n=7) were analyzed for each group.

2.4. SHED-T lymphocyte interaction analysis

To examine the apoptosis of SHED (passage 4) in the presence of T lymphocytes, 0.5×10^6 SHED were co-cultured with Pan-T cells for 3 days in six-well plates. Flow cytometric analysis (FACSCalibur, BD Bioscience) was utilized to evaluate SHED apoptosis utilizing Annexin V-PE Apoptosis Detection Kit (BD Bioscience). To analyze the role of the elasticity/porosity of the hydrogel biomaterial on SHED-T lymphocyte interaction *in vitro*, 2×10^6 SHED were encapsulated in 1 mL alginate hydrogel with different degrees of elasticity/porosity. The encapsulated SHED were co-cultured with (1×10^6) Pan-T cells for 3 days. After three days of co-culturing, the hydrogels were dissolved in sodium citrate buffer and apoptosis of SHED was evaluated according to the abovementioned method. Six independent specimens (n=6) were analyzed per group.

2.5. Osteo-differentiation of SHED *in vitro* and the role of inflammatory cytokines

5×10^5 SHED were cultured in a six-well plate under the osteogenic condition for 4 weeks while pro-inflammatory cytokines IFN-γ (50 ng/ml) and TNF-α (5 ng/ml) (BioLegend, San Diego CA) were added twice per week. Alizarin red staining was utilized after 4 weeks of osteo-induction. Additionally, to evaluate the role of the physiomechanical properties of alginate hydrogel, 2×10^6 SHED were encapsulated in 1 mL of alginate hydrogel with different porosity and elasticity. Encapsulated SHED were cultured under the osteogenic condition for 4 week [39–41]. Every 3 days, IFN-γ and TNF-α (BioLegend) were added to the culture for 4 weeks. Alizarin red staining was used to stain the specimens. Six specimens (n=6) were analyzed per group. Moreover, the samples were assayed using Western blot analysis to evaluate the influence of inflammatory cytokines in the activation of NF-kB pathway.

2.6. Western blot analysis

After 4 weeks of osteo-induction, MSCs were lysed using protein extraction buffer (Bio-Rad, Irvine, CA). The extracted proteins were fractionated in 10% sodium dodecyl sulfate-polyacrylamide gels (PAGE) and electrophoretically transferred to a nitrocellulose membrane (Bio-Rad). Next, the membranes were incubated with antibodies against RUNX2, ALP, and NF-kB (Abcam). *Beta-actin* (Abcam) was used as the housekeeping gene.

2.7. Regulation of MSC-host immune system cross-talk *in vivo*

Immunocompromised female 5-month old mice, (Beige nu/nu XIDIII, Harlan) or 5-month old wild type (C57BL/6, Harlan) mice were used in our animal study based on approved IACUC animal protocol by University of Southern California, Los Angeles (#10941).

4.0×10^6 SHED were encapsulated in alginate hydrogels, each containing 25 μg/ml rhBMP-2, with different degrees of elasticity. The MSC-scaffolds were subcutaneously implanted into the dorsal of either nude or wild type mice. Pan-T lymphocytes were isolated according to the methods reported previously [21,22]. 1×10^6 Pan-T lymphocytes, in 200 μL of PBS, were injected into the tail vein of nude mice instantly before the surgery. MSCs-scaffold constructs were implanted into nude mice subcutaneously (without Pan T injection) as positive controls, while the constructs without SHED were used as negative controls. Five animals (n=5) were used with four transplants in each.

The implanted MSCs in nude mice were harvested eight weeks post surgery and micro-CT analysis (MicroCAT II, Siemens Medical Solutions, Knoxville, TN) was preformed to analyze the amount of bone regeneration. Amira software (Visage Imaging Inc. San Diego, CA) was utilized to calculate BV/TV (bone volume/total volume). Additionally, to analyze the penetration of T-lymphocytes and apoptosis of the engrafted MSCs in wild type animals, 4.0×10^6 encapsulated SHED in alginate hydrogels, containing 25 μg/ml rhBMP-2, with different degrees of elasticity were subcutaneously implanted into the dorsal of wild type mice. Seven days post-surgery, the implanted MSCs were retrieved and immunofluorescently stained with antibodies against cleaved Caspase (cysteine-dependent aspartate-directed proteases)-3, -8, anti-NF-kB p65, and anti-Cox-2 antibodies. Five animals (n=5) were used with four transplants in each.

2.8. Histological, immunohistochemical and Immunofluorescence analysis

The retrieved tissue samples were prepared (fixed, paraffin embedded, and sectioned). Hematoxylin & Eosin staining was done on the prepared glass slides (H&E) (N=5 each group).

For immunohistochemical analysis, de-paraffinized sections were incubated with primary antibodies (anti-NF-kB p65 and anti-Cox-2 antibodies) for 1 h and detected using the universal immunoperoxidase (HRP) ABC kit (Vector Laboratories). They were counterstained with hematoxylin.

For immunofluorescence staining, the prepared specimens were stained with rabbit anti-Caspase-3 and Caspase-8 antibodies (Abcam) to detect the apoptosis of engrafted MSCs and were detected with Alexa Fluor 647 (red) and 488 (green) conjugated secondary antibody

(both 1:200 dilution). Subsequently, the specimens were counterstained with DAPI (Vector Laboratories, Burlingame, CA). The images were taken using a fluorescent microscope (Leica Microsystems, Buffalo Grove, IL).

2.9. Statistical analysis

The obtained data are presented as the mean ± standard deviation (SD). Kruskal-Wallis rank sum tests at a significance level of $\alpha = 0.05$ were used to evaluate the data. Whenever needed, two-tailed Student's t-tests were utilized.

3. Results

3.1. Characterization of the fabricated alginate hydrogel and permeability analysis

In the current study, SHED were isolated and encapsulated in an alginate hydrogel delivery system. Flow cytometric study was completed to evaluate the stemness of the isolated cells. Specific MSC markers including STRO-1 and CD146 were expressed by SHED (Supplementary Figure 1).

Figure 1a shows the elastic moduli of the alginate hydrogels, confirming that an increase in the calcium ion concentration increases the elasticity of the hydrogel. In addition, through light microscopy, it was determined that the fabricated alginate hydrogel microspheres were of uniform size (950 μm: average diameter), and had uniform MSC distribution (Figure 1b). Typically, a hydrogel scaffold should provide interconnected macropores to facilitate Oxygen and nutrient transfer to encapsulated cells. Here, the microstructures of alginate-based hydrogels formed in the presence of 100 mM and 200 mM calcium chloride concentrations were evaluated by various microscopic observations. SEM demonstrated that the hydrogels had an average pore size between 39.3 ±5.1 and 24.9 ±5.5 μm (Figure 1c and 1d). This is in good agreement with the reported values for alginate-based hydrogels in high calcium content.[42] However, It has to be mentioned that hydration of the hydrogel biomaterial might change the porosity of the lyophilized material. Our SEM examination showed that both fabricated hydrogels had a porous morphology. However, the alginate hydrogel with the greater elastic modulus (Alg200, 28–32 kPa) exhibited a smaller pore size (24.9 ±5.5 μm average pore diameter) and lower porosity (44.1%) in comparison to the softer hydrogel biomaterial with lower elastic modulus (18–24 kPa), which showed a larger pore size (39.3 ±5.1 μm average pore diameter) and higher degree of porosity (62.48%).

Taking into account the relationship between the mechanical properties and microstructure of the scaffolds and using the Theory of Elasticity[44], we also calculated the mesh size of the hydrogels, which were 29.2 nm and 33.6 nm for scaffolds with higher and lower elasticity, respectively.

Additionally, protein release profiles demonstrated that the elastic modulus of the alginate hydrogel, which affects its porosity, in turn, influences the release of the encapsulated protein molecules and therefore regulates the permeability of the scaffold (Figure 1e–g). Here we selected three different proteins to investigate how the size of macromolecules can affect their release. As shown in Figure 1e–g, Trypsin inhibitor (20 kDa; 4.8 nm in diameter), which was the smallest of the tested proteins, had the fastest release. The larger

protein BSA (66 kDa; 7.2 nm in diameter)[45] was released slower. IgG (150 kDa; 10.6 nm in diameter), the largest selected protein, was released slowest of all.

Although the mesh sizes of both of the hydrogels were large enough to allow diffusion of the encapsulated proteins, the more tortuous paths in the case of the tighter network (harder scaffold) significantly delayed the protein diffusion as it is seen in Figures 1e–1g. Additionally, as the size of the release protein was increased a more evident difference was observed ($P<0.05$) in the release profile between Alg100 (softer) and Alg200 (stiffer) hydrogels.

To further examine the role of the elasticity of the encapsulating biomaterial on the regulation of immune system, we evaluated the permeability of the utilized scaffolds possessing different elastic moduli against an inflammatory cytokine, TNF-α. Our immunofluorescence staining confirmed that the elasticity/porosity of the hydrogel controls the penetration of inflammatory cytokines. As expected, the scaffold with the higher degree of porosity demonstrated significantly faster diffusion of TNF-α within its matrix after 24 hours. (Figure 1h and 1i).

3.2. Characterization of the physiomechanical properties of biomaterials in SHED-immune interplay *in vitro*

SHED encapsulated within alginate scaffolds showed high degrees of viability after up to two weeks of being cultured in regular culture media (Figure 2a and 2b). Our FACS analysis showed that SHED underwent increased apoptosis upon being co-cultured with activated Pan-T cells for three days (Figure 2c). Interestingly, when SHED cells were encapsulated in alginate hydrogel microspheres, their apoptosis rate was significantly reduced. FACS data confirmed that the softer scaffold biomaterial with lower elasticity and higher porosity led to a higher number of apoptotic cells in comparison to the scaffold with higher elasticity and less porous structure (Figure 2c).

We have previously shown that pro-inflammatory cytokines can induce upregulation of the NF-kB pathway, leading to reduced bone regeneration capacity of encapsulated MSCs [22]. We further studied how the porosity and elasticity of the biomaterial encapsulating SHED can affect NF-kB pathway activity. Our Western blot analysis confirmed that IFN-γ and TNF-α activated the NF-kB pathway in SHED (Figure 2d). This phenomenon was diminished by encapsulating SHED cells in alginate hydrogel (Figure 2d). When encapsulated in alginate hydrogel down-regulation of NF-kB pathway activity was observed. This down-regulation of the NF-kB pathway was more pronounced when alginate hydrogel with higher elasticity was used, confirming that the elasticity and porosity of the biomaterial influence the MSC-host immune system cross-talk (Figure 2d).

The effects of pro-inflammatory cytokines on the down-regulation of SHED osteogenesis were also studied. After four weeks of osteo-induction in the presence of inflammatory cytokines (50 ng/ml IFN-γ and 5 ng/ml TNF-α), Alizarin red staining demonstrated reduced mineralization (Figure 3a). Also, Western blot analysis (after 2 weeks) showed down-regulation of expression levels of osteogenic regulators, confirming the inhibitory action of inflammatory cytokines on the osteogenesis of SHED *in vitro* (Figure 3d).

Furthermore, Xylenol orange staining and Western blot analysis exhibited that the alginate scaffold was capable of rescuing encapsulated SHED osteogenesis (Figure 3b and 3c). SHED encapsulated in alginate hydrogel with greater elasticity and less porosity showed modest expression levels of osteogenic markers, while SHED encapsulated in softer alginate (with higher porosity) exhibited lower expression levels of osteogenic markers (Figures 3d).

3.3. Analysis of the effects of elasticity and porosity of the biomaterial on osteogenesis of SHED *in vivo*

In this study, 4×10^6 SHED were encapsulated in 1 mL alginate hydrogel with different degrees of porosity/elasticity and were implanted into immunocompromised and wild type mice subcutaneously. 1×10^6 Pan T lymphocytes were isolated and injected into the tail vein of the immunocompromised mice immediately prior to the surgical procedure. Micro-CT and histological analyses revealed that encapsulating SHED in alginate hydrogel with a greater elastic modulus led to a larger amount of bone regeneration in comparison to cells encapsulated in a more porous scaffold with lower elasticity (Figure 4 a–d). Figures 4c and 4d exhibit the semi-quantified micro-CT and histological data, respectively. The positive control group (encapsulated SHED in alginate 100 in nude mice) generated the largest amount of bone formation, while the negative control group (cell-free alginate) failed to generate any bone ($p < 0.05$). Our findings confirmed the inhibitory effects of pro-inflammatory T cells and the role oh hydrogel characteristics on the fate of engrafted cells.

To further characterize the role of the biomaterial's mechanical properties and microarchitecture in SHED-host immune interplay, 4×10^6 encapsulated SHED were subcutaneously implanted in wild type mice and SHED apoptosis was evaluated at one week post-implantation. The harvested specimens were immunohistochemically stained against anti-Cox-2 and anti-NF-kB p65 antibodies. Our results (Figure 5a) revealed greater amounts of positive immunostaining for anti-Cox-2 and anti-NF-kB p65 antibodies in SHED within more porous hydrogel with lower elasticity compared to the cells encapsulated in the denser alginate hydrogel with greater elasticity (Figure 5a), confirming that less SHED underwent apoptosis in the denser biomaterial. Additionally, our immunofluorescence analysis demonstrated higher expression levels of Caspase-3 and -8 in encapsulated SHED in softer (more porous) alginate hydrogel compared to SHED encapsulated in a more rigid alginate hydrogel with a lower degree of porosity (Figure 5b and 5c).

4. Discussion

Our research group and others have reported that inflammatory T-lymphocytes from the host are capable of prevention of osteo-differentiation of implanted MSCs *via* IFN-γ-mediated downregulation of osteogenesis and upregulation of TNF-α signaling, leading to cell apoptosis [21, 22]. Additionally, it has been shown that encapsulating cells in alginate hydrogel can retard the infiltration of proinflammatory T cells and cytokines by acting as a physical barrier, and therefore buffer the implanted MSCs from the attack of the host immune system [22]. These discoveries demonstrate that the encapsulating biomaterial affect the cross-talk between MSC and host immune cells, regulate the viability and osteogenesis of the implanted MSCs, and improve tissue regeneration quality. Our research

group and others have confirmed that modifying the elasticity of a hydrogel biomaterial can be used to regulate stem cell lineage differentiation in 3D cultures [22, 24, 39]. However, there are no studies evaluating the role of physiomechanical properties (e.g., porosity and elasticity) of the biomaterial in the interplay between MSCs and proinflammatory T cells/cytokines. To develop effective MSC-based regenerative therapies, it is crucial to have a clear understanding of how the encapsulating hydrogel biomaterial's physiomechanical properties affect the MSCs-host immune system cross-talk. In this study SHED were utilized to investigate this phenomenon. Dental-derived MSCs are very appealing for craniofacial tissue engineering applications, since they may be more committed to differentiate into craniofacial structures [11–15]. The suitability of SHED for bone tissue engineering has been established [15,16]. SHED are easily available in our pediatric patients' mouth and can be found in biological waste in pediatric dental clinics [15,16]. Considering the neural crest-derived origin of the dental pulp, SHED can play an important role in the development and formation of various craniofacial tissues including craniofacial bone, which are also of neural crest origin [16].

Our studies have demonstrated that SHED represent a population of postnatal stem cells capable of extensive proliferation and multipotential differentiation (data not shown). Therefore, SHED provide a promising cell source for bone tissue engineering applications. However, the interaction of these cells with the host immune system and the significance of the encapsulating biomaterial remains to be determined. Therefore, in the current study, SHED were isolated form the pulp of teeth from children aged 6–12 years and were encapsulated in RGD-modified alginate hydrogel scaffolds with two different elastic moduli (18–24 KPa vs 28–32 KPa) and porosity (39.3 vs 24.9 μm average pore diameter).

Our *in vitro* studies confirmed that upon increasing the elasticity of the hydrogel scaffold, it becomes denser, with decreased pore size and porosity. This decrease in the pore size was able to delay the release of proteins with dissimilar molecular weights from the hydrogel in a size-dependent manner. Additionally, it delayed the infiltration of TNF-alpha (a pro-inflammatory cytokine) within the hydrogel matrix. These data confirmed that elasticity/porosity of the alginate hydrogel can control the diffusion rate and permeability. Moreover, encapsulating SHED cells within hydrogel protected them from T-cell induced apoptosis and preserved their osteogenic differentiation. However, the observed effect was more pronounced when the cells were encapsulated in a hydrogel with greater elasticity. Our findings therefore demonstrate that the alginate hydrogel biomaterial's elasticity and porosity can readily regulate MSC-host immune system interplay.

Our findings prompted us to examine whether the elasticity and the microstructure of the encapsulating hydrogel biomaterial can regulate the apoptosis of the encapsulated SHED by controlling the activity of the NF-kB pathway. NF-κB is a major transcription factor, which regulates innate and adaptive immunity. It is well known that, the nuclear factor NF-κB (NF-kB) pathway is one of the main moderators of inflammatory processes by upregulting the expression levels of proinflammatory cytokines (e.g. TNFα) [46]. Moreover, studies have shown that, NF-kB pathway is capable of upregulating COX-2 pathway activation [47] In the current study, we revealed down-regulation of Cox-2 and NF-kB p65 expression in encapsulated SHED in alginate hydrogel with greater elasticity and less porosity.

Our *in vivo* studies exhibited that host pro-inflammatory T-lymphocytes can prevent SHED-mediated osteogenesis in our animal model in nude mice. Pan-T infusion inhibited the SHED-mediated bone regeneration in these mice. However, our results clearly demonstrate that the porosity and the elasticity of the hydrogel scaffold used to encapsulate the SHED can regulate this cross talk and enhance the quality of the bone tissue regeneration. In order to corroborate our findings, encapsulated SHED were implanted subcutaneously in wild type mice and after one week of implantation, the infiltration of T-lymphocytes and presence of apoptotic SHED inside the hydrogel constructs were analyzed. Our findings showed that the porosity of the hydrogel biomaterial controlled the apoptosis of implanted SHED through regulation of the diffusion of inflammatory T-cells into the engrafted MSC-hydrogel constructs. Altogether, the obtained results confirm that scaffold can regulate inflammatory T-lymphocyte-induced apoptosis of encapsulated SHED, and that the physiomechanical properties (porosity and elasticity) of the hydrogel help to determine the viability and fate of the engrafted MSCs.

5. Conclusions

Here, we demonstrate that the porosity and elasticity of the encapsulating hydrogel biomaterial play an important role in dental-derived MSC-immune cell interplay and therefore in MSC viability and fate determination. Our findings suggest that the physical properties and microarchitecture of the encapsulating hydrogel biomaterial regulate the permeation of pro-inflammatory cytokines and T-lymphocytes and therefore osteogeneiss of MSCs. These findings might lead to development of an innovative treatment approach for high quality MSC-mediated bone tissue engineering.

Supplementary Material

Refer to Web version on PubMed Central for supplementary material.

Acknowledgments

Authors (S.A. and A.M.) would like to thank Prof. Ali Khademhosseini for his critical review of the manuscript. This work was supported by the National Institutes of Health (K08DE023825 to A.M. and K99E025915 to C.C.).

References

1. Sachlos E, Czernuszka JT. Making tissue engineering scaffolds work. Review on the application of solid freeform fabrication technology to the production of tissue engineering scaffold. European Cells and Materials. 2003; 5:29–40. [PubMed: 14562270]
2. Monaco E, Bionaz M, Hollister SJ, Wheeler MB. Strategies for regeneration of the bone using porcine adult adipose-derived mesenchymal stem cells. Theriogenology. 2011; 75:1381–99. [PubMed: 21354606]
3. Chen FM, Zhang J, Zhang M, An Y, Chen F, Wu ZF. A review on endogenous regenerative technology in periodontal regenerative medicine. Biomaterials. 2010; 31:7892–7927. [PubMed: 20684986]
4. Caplan AI. Adult mesenchymal stem cells for tissue engineering versus regenerative medicine. J Cell Physiol. 2007; 213:341–347. [PubMed: 17620285]
5. García-Gómez I, Elvira G, Zapata AG, Lamana ML, Ramirez M, Garcia Castro J, Garcia Arranz M, Vicente J, Bueren J, Garcia-Olmo D. Mesenchymal stem cells: biological properties and clinical applications. Expert Opin Biol Ther. 2010; 10:1453–1468. [PubMed: 20831449]

6. Tasso R, Fais F, Reverberi D, Tortelli F, Cancedda R. The recruitment of two consecutive and different waves of host stem/progenitor cells during the development of tissue-engineered bone in a murine model. Biomaterials. 2010; 31:2121–2129. [PubMed: 20004968]
7. Chung IH, Yamaza T, Zhao H, Choung PH, Shi S, Chai Y. Stem cell property of post migratory cranial crest cells and their utility in alveolar bone regeneration and tooth development. Stem Cells. 2009; 27:866–877. [PubMed: 19350689]
8. Caplan AI. Mesenchymal stem cells. J Orthop Res. 1991; 9:641–650. [PubMed: 1870029]
9. Friedenstein AJ, Chailakhjan RK, Lalykina KS. The development of fibroblast colonies in monolayer cultures of guinea-pig bone marrow and spleen cells. Cell Tissue Kinet. 1970; 3:393–403. [PubMed: 5523063]
10. Bi Y, Ehirchiou D, Kilts TM, Inkson CA, Embree MC, Sonoyama W, Li L, Leet AI, Seo B-M, Zhang L, Shi S, Young MF. Identification of tendon stem/progenitor cells and the role of the extracellular matrix in their niche. Nat Med. 2007; 13:1219–1227. [PubMed: 17828274]
11. Batouli S, Miura M, Brahim J, Tsutsui TW, Fisher LW, Gronthos S, Robey PG, Shi S. Comparison of stem cell–mediated osteogenesis and dentinogenesis. J Dent Res. 2003; 82:976–981. [PubMed: 14630898]
12. Tomar GB, Srivastava RK, Gupta N, Barhanpurkar AP, Pote ST, Jhaveri HM, Mishra GC, Wani MR. Human gingiva-derived mesenchymal stem cells are superior to bone marrow-derived mesenchymal stem cells for cell therapy in regenerative medicine. Biochemistry Biophysics Research Communications. 2010; 393:377–383.
13. Lindroos B, Maenpaa K, Ylikomi T, Oja H, Suuronen R, Miettinen S. Characterization of human dental stem cells and buccal mucosa fibroblasts. Biochemistry Biophysics Research Communications. 2008; 368:329–335.
14. Zhang Q, Shi S, Liu Y, Uyanne J, Shi Y, Shi S, Le AD. Mesenchymal Stem Cells Derived from Human Gingiva Are Capable of Immunomodulatory Functions and Ameliorate Inflammation-Related Tissue Destruction in Experimental Colitis. Journal of Immunology. 2009; 183:7787–7798.
15. Miura M, Gronthos S, Zhao M, Lu B, Fisher LW, Robey PG, Shi S. SHED: Stem cells from human exfoliated deciduous teeth. PNAS. 2003; 100:5807–5812. [PubMed: 12716973]
16. Seo BM, Sonoyama W, Yamaza T, Coppe C, Kikuiri T, Akiyama K, Lee JS, Shi S. SHED repair critical-size calvarial defects in mice. Oral Dis. 2008; 14(5):428–34. [PubMed: 18938268]
17. Chadipiralla K, Yochim JM, Bahuleyan B, Huang CY, Garcia-Godoy F, Murray PE, Stelnicki EJ. Osteogenic differentiation of stem cells derived from human periodontal ligaments and pulp of human exfoliated deciduous teeth. Cell Tissue Res. 2010; 340:323–33. [PubMed: 20309582]
18. Zhang QZ, Nguyen AL, Yu WH, Le AD. Human oral mucosa and gingiva: a unique reservoir for mesenchymal stem cells. J Dent Res. 2012; 91:1011–8. [PubMed: 22988012]
19. Sun L, Akiyama K, Zhang H, Yamaza T, Hou Y, Zhao S, Xu T, Le A, Shi S. Mesenchymal stem cell transplantation reverses multi-organ dysfunction in systemic lupus erythematosus mice and humans. Stem Cells. 2009; 27:1421–1432. [PubMed: 19489103]
20. Akiyama K, Chen C, Wang D, Xu X, Qu C, Yamaza T, Cai T, Chen W, Sun L, Shi S. Mesenchymal-stem-cell-induced immunoregulation involves FAS-ligand-/FAS-mediated T cell apoptosis. Cell Stem Cell. 2012; 10:544–55. [PubMed: 22542159]
21. Liu Y, Wang L, Kikuiri T, Akiyama K, Chen C, Xu X, Yang R, Chen WJ, Wang S, Shi S. Mesenchymal stem cell-based tissue regeneration is governed by recipient T lymphocytes via IFN-gamma and TNF-alpha. Nat Med. 2011; 17:1594–1601. [PubMed: 22101767]
22. Moshaverinia A, Chen C, Xu X, Ansari S, Zadeh HH, Schricker SR, Moradian-Oldak J, Khademhosseini A, Snead ML, Shi S. Regulation of the Stem Cell-Host Immune System Interplay Using Hydrogel Coencapsulation System with an Antiinflammatory Drug. Adv Func Mater. 2015; 25(15):15. 2296–2307.
23. Pumberger M, Qazi TH, Ehrentraut MC, Textor M, Kueper J, Stoltenburg-Didinger G, Winkler T, von Roth P, Reinke S, Borselli C, Perka C, Mooney DJ, Duda GN, Geißler S. Synthetic niche to modulate regenerative potential of MSCs and enhance skeletal muscle regeneration. Biomaterials. 2016 Aug.99:95–108. DOI: 10.1016/j.biomaterials.2016.05.009 [PubMed: 27235995]

24. Engler AJ, Sen S, Sweeney HL, Discher DE. Matrix elasticity directs stem cell lineage specification. Cell. 2006; 126:677–689. [PubMed: 16923388]
25. Kretlow JD, Young S, Klouda L, Wong M, Mikos AG. Injectable biomaterials for regenerating complex craniofacial tissues. Adv Mater. 2009; 21:3368–79. [PubMed: 19750143]
26. Hill E, Boontheekul T, Mooney DJ. Designing scaffolds to enhance transplanted myoblast survival and migration. Tissue Eng. 2006; 12:1295–1302. [PubMed: 16771642]
27. Rowley JA, Madlambayan G, Mooney DJ. Alginate hydrogels as synthetic extracellular matrix materials. Biomaterials. 1999; 20:45–51. [PubMed: 9916770]
28. Gautier A, Carpentier B, Dufresne M, Vu Dinh Q, Paullier P, Legallais C. Impact of alginate type and bead diameter on mass transfer and the metabolic activities of encapsulated C3A cells in bioartificial liver applications. Eur Cell Mater. 2011; 21:94–106. [PubMed: 21267945]
29. Gronowicz GA, Derome ME. Synthetic peptide containing Arg-Gly-Asp inhibits bone formation and resorption in a mineralizing organ culture system of fetal rat parietal bones. J Bone Miner Res. 1994; 9:193. [PubMed: 8140932]
30. Xiao G, Wang D, Benson MD, Karsenty G, Franceschi RT. Role of the alpha 2-integrin in osteoblast-specific gene expression and activation of the Osf2 transcription factor. J Biol Chem. 1998; 273:32988. [PubMed: 9830051]
31. Ruoslahti E, Pierschbacher MD. Arg-Gly-Asp: a versatile cell recognition signal. Cell. 1986; 44:517. [PubMed: 2418980]
32. Wang CC, Yang KC, Lin KH, Liue HC, Lin FH. A highly organized three-dimensional alginate scaffold for cartilage tissue engineering prepared by microfluidic technology. Biomater. 2011; 32:7118–7126.
33. Moshaverinia A, Chen C, Akiyama K, Ansari S, Xu X, Chee WW, Schricker SR, Shi S. Alginate hydrogel as a promising scaffold for dental-derived stem cells: an in vitro study. J Mater Sci: Mater Med. 2012; 23:3041–3051. [PubMed: 22945383]
34. Moshaverinia A, Chen C, Akiyama K, Xu X, Chee WW, Schricker SR, Shi S. Encapsulated dental-derived mesenchymal stem cells in an injectable and biodegradable scaffold for applications in bone tissue engineering. J Biomed Mater Res A. 2013; 101:3285–94. [PubMed: 23983201]
35. Sapir Y, Kryukov O, Cohen S. Integration of multiple cell-matrix interactions into alginate scaffolds for promoting cardiac tissue regeneration. Biomaterials. 2011; 7:1838–47.
36. Mao AS, Shin JW, Mooney DJ. Effects of substrate stiffness and cell-cell contact on mesenchymal stem cell differentiation. Biomaterials. 2016; 98:184–191. [PubMed: 27203745]
37. Moshaverinia A, Ansari S, Chen C, Xu X, Akiyama K, Snead ML, Zadeh HH, Shi S. Co-encapsulation of anti-BMP2 monoclonal antibody and mesenchymal stem cells in alginate microspheres for bone tissue engineering. Biomaterials. 2013; 34:6572–9. [PubMed: 23773817]
38. Moshaverinia A, Chen C, Xu X, Akiyama K, Ansari S, Zadeh HH, Shi S. Bone regeneration potential of stem cells derived from periodontal ligament or gingival tissue sources encapsulated in RGD-modified alginate scaffold. Tissue Eng Part A. 2014 Feb; 20(3–4):611–21. [PubMed: 24070211]
39. Chaudhuri O, Koshy ST, Branco da Cunha C, Shin JW, Verbeke CS, Allison KH, Mooney DJ. Extracellular matrix stiffness and composition jointly regulate the induction of malignant phenotypes in mammary epithelium. Nat Mater. 2014 Oct; 13(10):970–8. [PubMed: 24930031]
40. Horniblow RD, Dowle M, Iqbal TH, Latunde-Dada GO, Palmer RE, Pikramenou Z, Tselepis C. Alginate-Iron Speciation and Its Effect on In Vitro Cellular Iron Metabolism. PLOS ONE. 2015; 10:e0138240. [PubMed: 26378798]
41. Saggiomo V, Velders AH. Simple 3D Printed Scaffold-Removal Method for the Fabrication of Intricate Microfluidic Devices. Advanced Science. 2015; 2:1500–125.
42. Lee KY, Mooney DJ. Alginate: Properties and biomedical applications. Progress in Polymer Science. 2012; 37:106–26. [PubMed: 22125349]
43. Thevenot P, Nair A, Dey J, Yang J, Tang L. Method to analyze three-dimensional cell distribution and infiltration in degradable scaffolds. Tissue Engineering Part C: Methods. 2008; 14:319–31. [PubMed: 19055358]
44. Gardel ML, Shin JH, MacKintosh FC, Mahadevan L, Matsudaira P. Elastic behavior of cross-linked and bundled actin networks. Science. 2004; 304:1301–1305. [PubMed: 15166374]

45. Koutsopoulos S, Unsworth L, Larry D, Nagai Y, Zhang S. Controlled release of functional proteins through designer self-assembling peptide nanofiber hydrogel scaffold. Proc Natl Acad Sci U S A. 2009; 106:4623–4628. [PubMed: 19273853]

46. Jung YJ, Isaacs JS, Lee S, Trepel J, Neckers L. IL-1beta-mediated upregulation of HIF-1alpha via an NFkappaB/COX-2 pathway identifies HIF-1 as a critical link between inflammation and oncogenesis. FASEB J. 2003; 17:2115–7. [PubMed: 12958148]

47. Nakao S, Ogtata Y, Shimizu E, Yamazaki M, Furuyama S, Sugiya H. Tumor necrosis factor alpha (TNF-alpha)-induced prostaglandin E2 release is mediated by the activation of cyclooxygenase-2 (COX-2) transcription via NFkappaB in human gingival fibroblasts. Mol Cell Biochem. 2002; 238:11–8. [PubMed: 12349897]

Statement of Significance

In this study, we demonstrate that alginate hydrogel regulates the viability and the fate of the encapsulated dental-derived MSCs through modulation of NF-kB pathway. Alginate hydrogels with smaller pores and higher elasticity prevent pro-inflammatory cytokine-induced MSC apoptosis by down-regulating the Caspase-3- and 8- associated proapoptotic cascade, leading to higher amounts of ectopic bone regeneration. MSCs encapsulated in hydrogel with higher elasticity exhibited lower expression levels of NF-kB p65 and Cox-2 *in vivo*. These findings confirm that the fate of encapsulated MSCs are affected by the stiffness and microarchitecture of the encapsulating hydrogel biomaterial, as well as presence of T-lymphocytes/pro-inflammatory cytokines providing evidence concerning material science, stem cell biology, the molecular mechanism of dental-derived MSC-associated therapies, and the potential clinical therapeutic impact of MSCs.

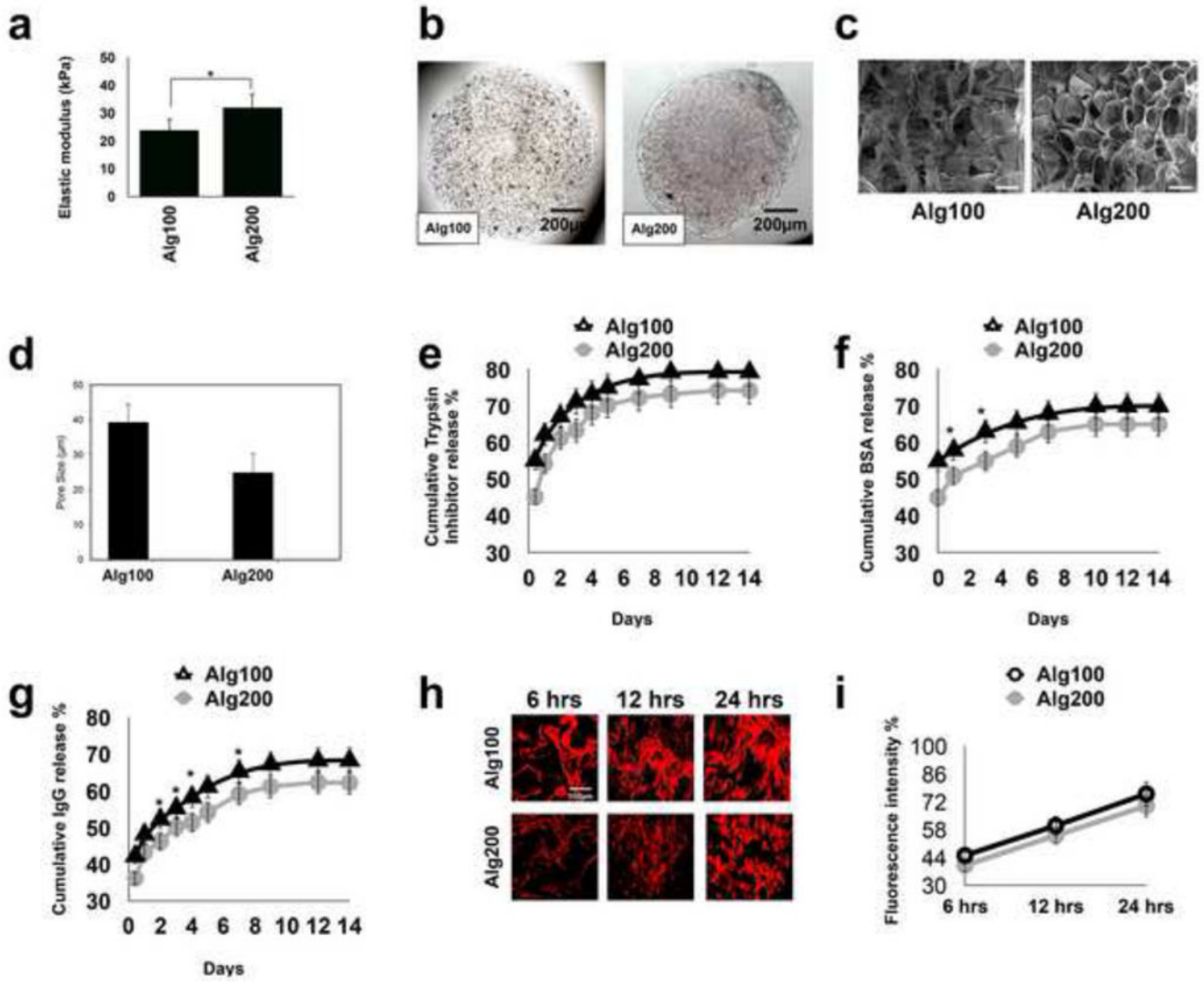

Figure 1. Characterization of the developed hydrogel biomaterials

(a) The modulus of elasticity of the fabricated alginate hydrogels in the presence of two different concentrations of calcium ions (100 and 200 mM, showing increased elasticity in presence of a higher concentration of calcium. (b) Light microscopic images of the fabricated microspheres. (c) SEM micrographs of prepared hydrogels at the two different calcium ion concentrations. (d) The calculated average pore size for the two different hydrogels based on SEM images. *In vitro* trypsin inhibitor (e), BSA (f), and IgG (g) release profile from alginate hydrogels with different elastic moduli/porosity showing decreased release amounts from alginate hydrogel with greater stiffness. (h, i) Qualitative and quantitative characterization of the permeability of fabricated alginate microspheres to TNF-α using immunofluorescence staining, showing reduced infiltration of TNF-α in alginate hydrogel with greater elasticity and lower porosity. Scale bar: c, 30 μm; *P<0.05.

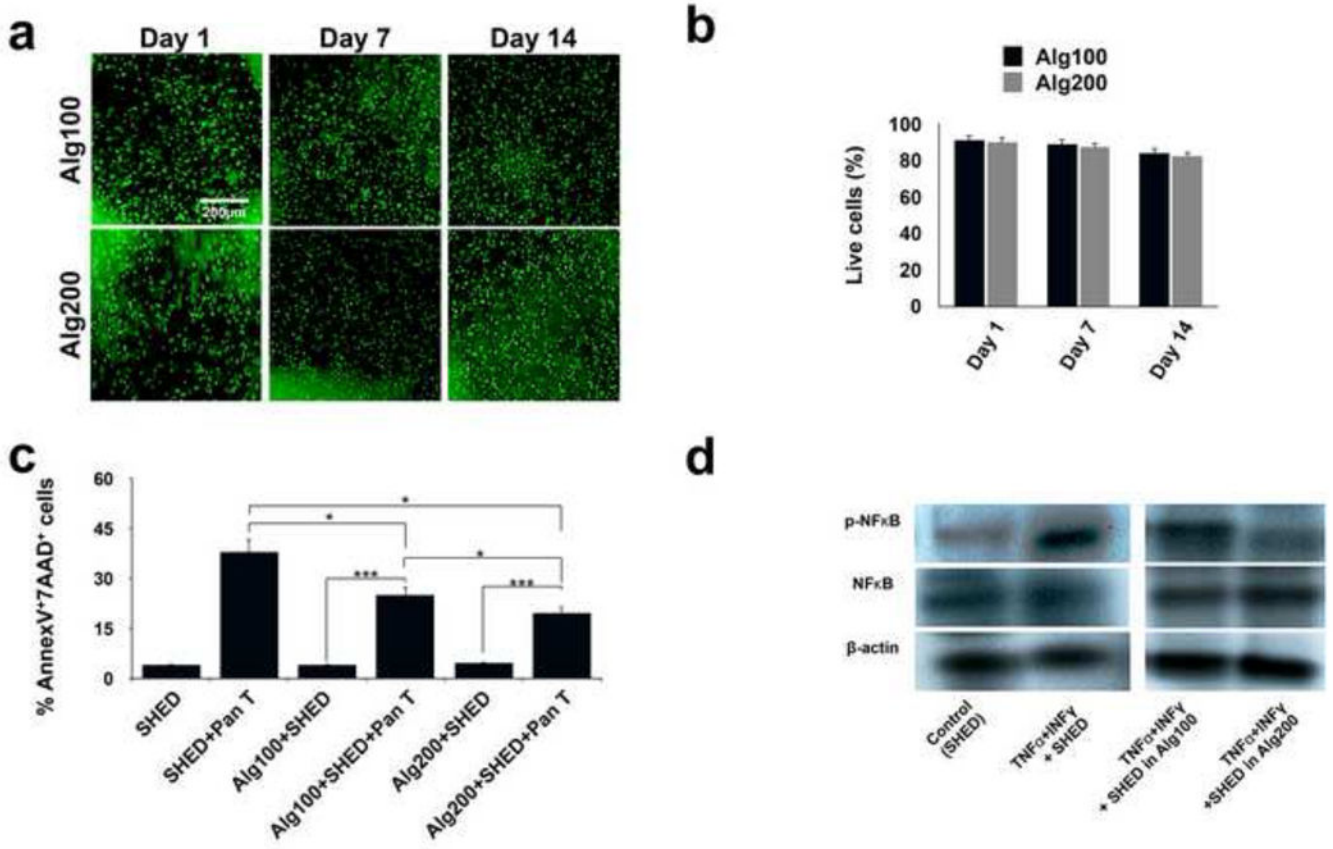

Figure 2. Biomaterial physical properties and microarchitecture affect SHED-immune system interplay *in vitro*

(a) Live/dead staining of encapsulated SHED MSCs in fabricated hydrogels after two weeks of culturing in regular media (scale bar = 200 mm). (b) Viability of the encapsulated MSCs: percentage of live MSCs in alginate microspheres with different elasticity/porosity. (c) Apoptosis of SHED in the presence of activated Pan-T lymphocytes after three days of co-culturing, as confirmed by FACS analysis using Annexin V-FITC apoptosis detection kit. The protective properties of encapsulating biomaterials and the role of their porosity/elasticity were demonstrated by the reduced apoptosis of encapsulated SHED in the presence of activated Pan-T lymphocytes after three days of co-culturing, as confirmed by FACS analysis using an Annexin V-FITC apoptosis detection kit. (d) Western blot analysis showed upregulation of the NF-kB pathway in SHED in the presence of IFN-γ (50 ng/ml) and TNF-α (5 ng/ml), showing the harmful effects of pro-inflammatory cytokines on MSC survival. Encapsulating SHED in alginate hydrogel with higher elasticity (lower porosity) down-regulated NF-kB pathway activity relative to that of SHED encapsulated in more porous alginate hydrogel. *P<0.05, ***P<0.001.

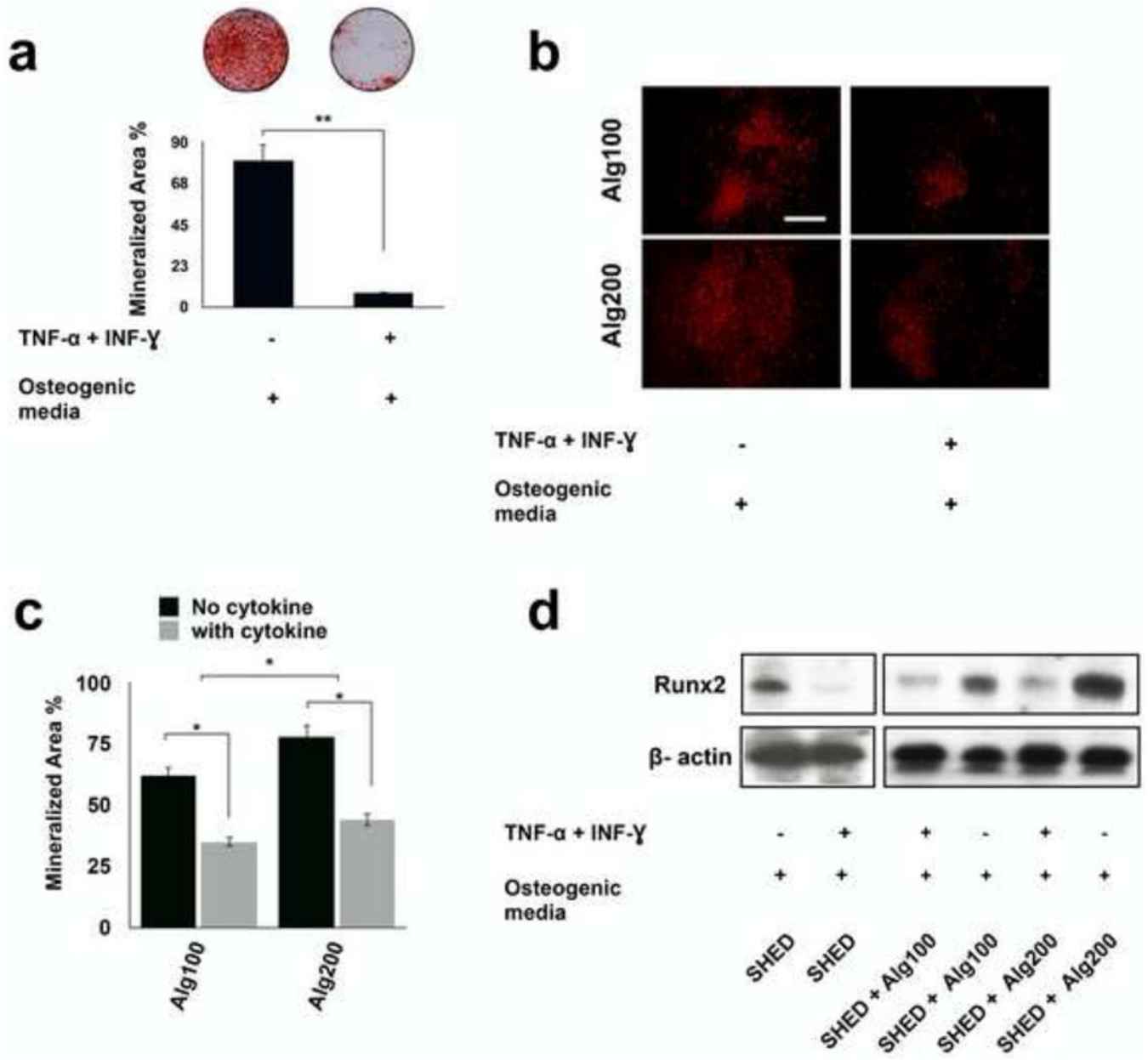

Figure 3. Down-regulation of SHED osteogenesis in the presence of pro-inflammatory cytokines

(a) Alizarin red staining showed reduced mineralized nodule formation for SHED cultured in osteogenic media in the presence of IFN-γ 50 (ng m/l)- TNF-α (5 ng m/L) combination. Mineralization area percentage was defined as the area of stained mineralization divided by the total area. (b) The protective role of the biomaterial was confirmed by osteogenic differentiation of encapsulated SHED in alginate with different degrees of elasticity/porosity in the presence of IFN-γ and TNF-α for 4 weeks and staining with Xylenol orange fluoroprobe. (c) Mineralization area percentage was defined as the area of stained mineralization divided by the total area of the field of view of the image in d. (d) Western blot analysis showed that pro-inflammatory cytokine-treated SHED expressed decreased levels of osteogenic marker. Moreover, Western blot analysis confirmed that the

physiomechanical properties of the encapsulating hydrogel biomaterial regulated the expression of osteogenic marker levels (RUNX2) in the presence of IFN-γ and TNF-α. NS= not significant, *P<0.05, **P<0.01.

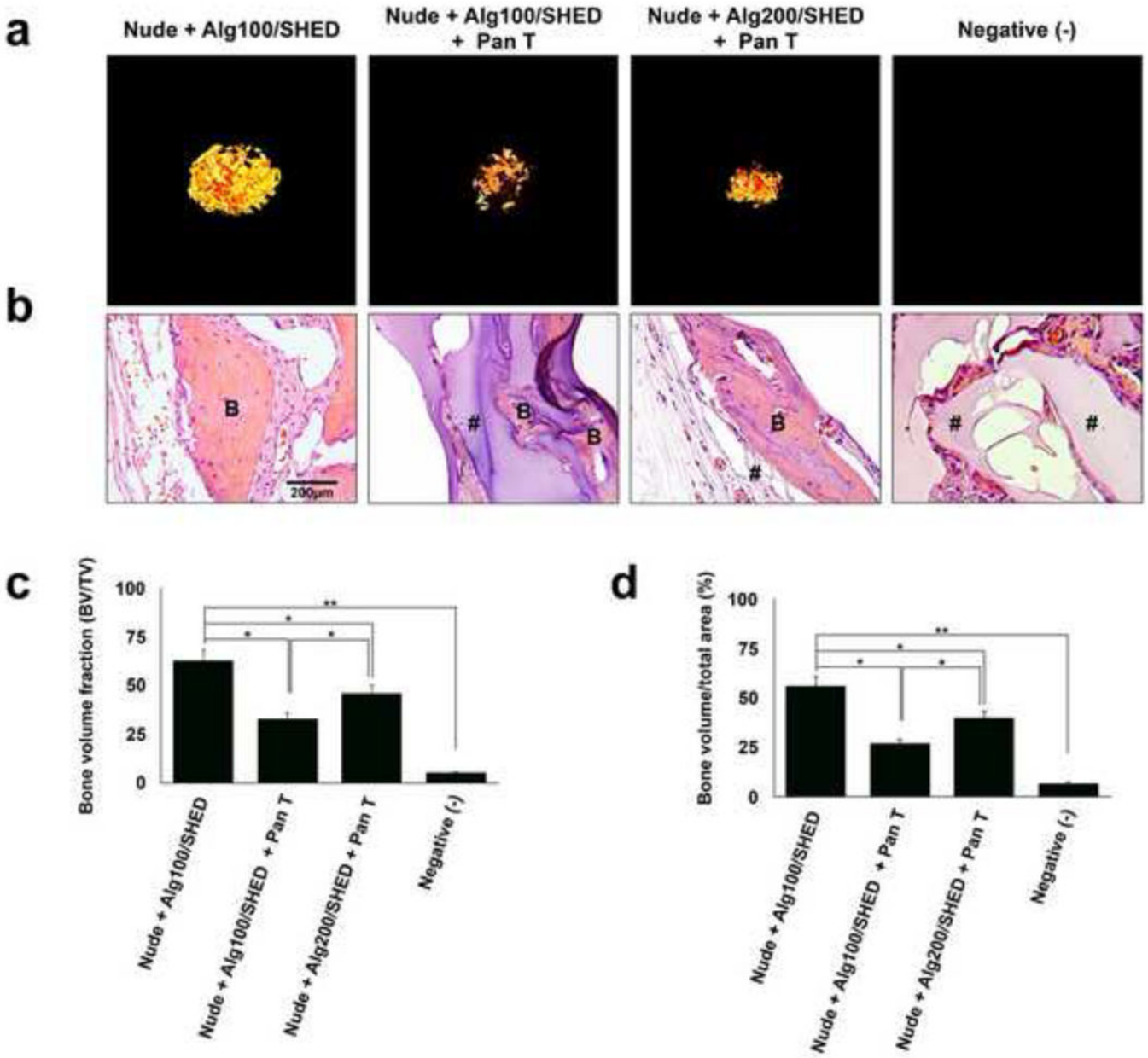

Figure 4. Biomaterial-T lymphocyte cross-talk regulates SHED-mediated bone regeneration

(a) Micro-CT images of SHED encapsulated in alginate hydrogels with different physiomechanical properties, retrieved 8 weeks after subcutaneous implantation in immunocompromised mice. Pan T lymphocytes were isolated and injected into the mice via the tail vein immediately prior to the surgical procedures. (b) Histological analysis (H&E staining) of retrieved specimens after 8 weeks of subcutaneous implantation. (c) Semi-quantitative analysis via micro-CT images (a) showing the bone volume fraction (BV/TV). (d) Semi-quantitative analysis of the amount of bone regeneration from histological slide presented in panel b. B: regenerated bone, #: connective tissue. NS= not significant, *P<0.05, **P<0.01.

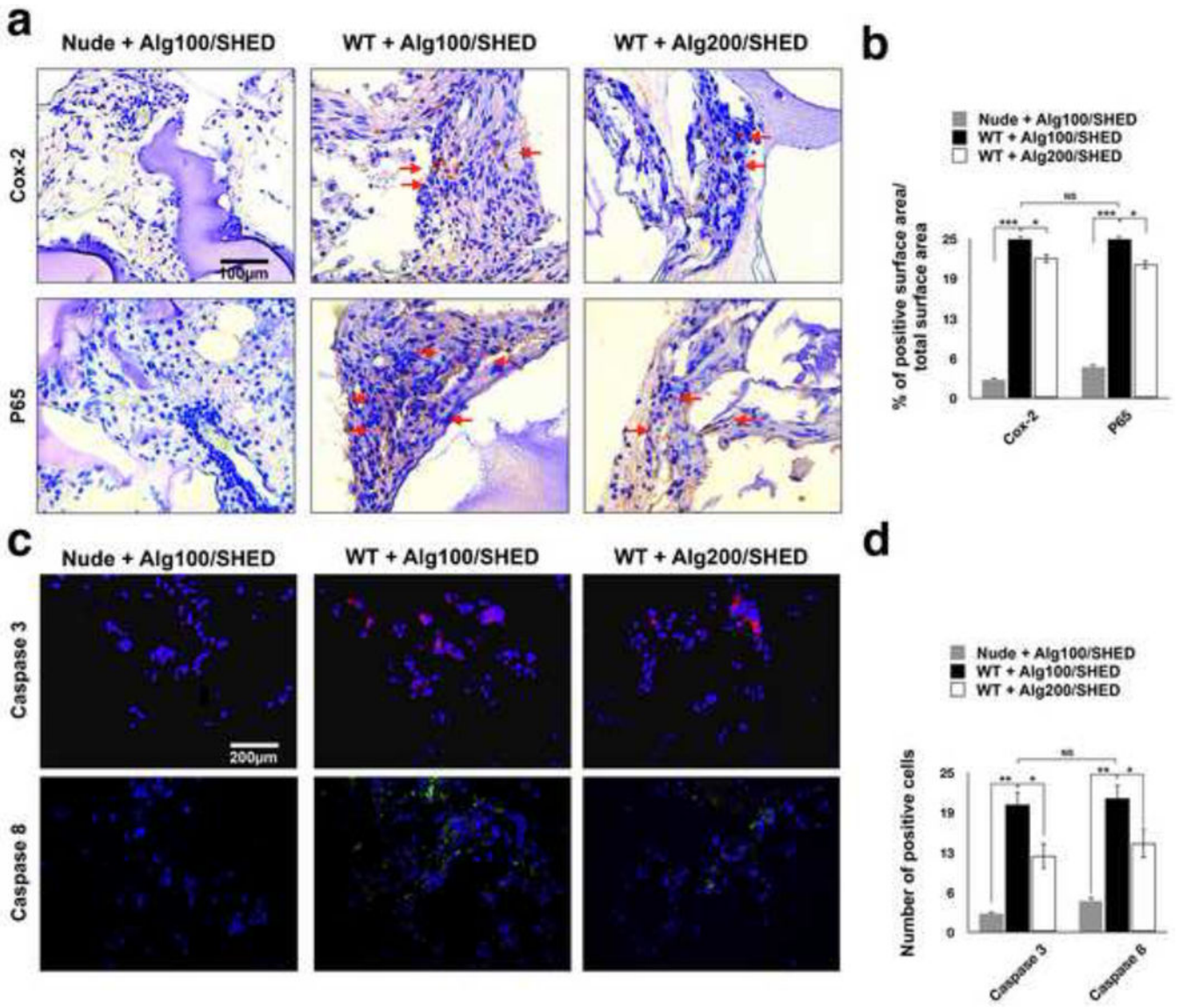

Figure 5. Post-implantation characterization of implanted MSCs

To further analyze the role of the physiomechanical properties of the encapsulating biomaterial on MSC-immune system cross-talk, the encapsulated SHED cells were subcutaneously implanted in wild type mice and SHED apoptosis was evaluated 1 week post-implantation. Encapsulated SHED in alginate hydrogel implanted in nude mice were used as the control. (a) Immunohistochemical staining with antibodies against anti-NF-kB p65 and anti- Cox-2 antibodies of specimens retrieved after one week of implantation showing higher expression levels of (upper panel) Cox-2 and (lower panel) NF-kB p65 (red arrows) in encapsulated SHED in alginate hydrogel with lower elasticity and greater porosity. (b) Semi-quantitative analysis of the percentage of positive surface area in panel a. (c) Fluorescent immuno-staining with antibodies against Caspase-3 (upper panel) and Caspase-8 (lower panel) after 1 week of implantation revealing significantly higher expression levels of Caspase-3 and Caspase-8 in encapsulated SHED in alginate hydrogel

with lower elasticity and greater porosity. (d) Semi-quantitative analysis of the number of positive cells in panel c. NS= not significant, *P<0.05, **P<0.01.